Vis Comput
DOI 10.1007/s00371-009-0340-6

ORIGINAL ARTICLE

Salient spectral geometric features for shape matching and retrieval

Jiaxi Hu · Jing Hua

Abstract This paper introduces a new method for extracting salient features from surfaces that are represented by triangle meshes. Our method extracts salient geometric feature points in the Laplace–Beltrami spectral domain instead of usual spatial domains. Simultaneously, a spatial region is determined as a local support of each feature point, which is correspondent to the "frequency" where the feature point is identified. The local shape descriptor of a feature point is the Laplace–Beltrami spectrum of the spatial region associated to the points which are stable and distinctive. Our method leads to the salient spectral geometric features invariant to spatial transforms such as translation, rotation, and scaling. The properties of the discrete Laplace–Beltrami operator make them invariant to isometric deformations and mesh triangulations as well. With the scale information transformed from the "frequency", the local supporting region always maintains the same ratio to the original model no matter how it is scaled. This means that the spatial region is scale-invariant as well. Therefore, both global and partial matching can be achieved with these salient feature points. We demonstrate the effectiveness of our method with many experiments and applications.

Keywords Shape matching · Spectral geometry · Geometric analysis

J. Hu · J. Hua (✉)
Department of Computer Science, Wayne State University, Detroit, MI 48202, USA
e-mail: jinghua@wayne.edu

J. Hu
e-mail: jiaxihu@wayne.edu

Published online: 03 March 2009

1 Introduction

Shape matching is a fundamental problem in many research fields, such as computer graphics, vision, image processing, robotics, and so on. In the recent years, the advancement of scanning techniques makes it easier and faster to produce massive 3D surface data. Subsequently, matching, searching, and retrieval for 3D surface shapes is getting increasingly important. However, 3D surfaces have many unique spatial factors such as translation, rotation, and scaling [12]. Their shape can also be deformed [15]. On the other hand, because of their efficiency in rendering and storage, triangle or polygonal meshes are widely used for 3D surface representation, but their irregular sampling also brings problems to analysis. All these issues make 3D surface shape matching a very challenging task, which largely relies on a powerful shape representation.

This paper describes a method to represent a shape with a set of salient features. The shapes are presented with triangle meshes without any pre-process such as normalization or alignment. The features are extracted in the Laplace–Beltrami spectrum domain instead of the shape's spatial domain. As a result, the salient features are invariant to the spatial translation, rotation, and scaling. They are also invariant to isometric deformations, as the Laplace–Beltrami spectrum is an isometric invariant [20]. Because the discrete Laplace–Beltrami operator is applied on meshes, the spectrum is invariant to the different sampling rates and triangulations of the meshes as well. Our method extracts not only the location of each feature point but also the "frequency" where the feature point lies. The "frequency" information can imply a spatial scale to define a local region supporting the feature point. Since the spectrum is invariant, the region is an "absolute" shape, i.e., invariant to those transformations. We employ the Laplace–Beltrami spectrum again on

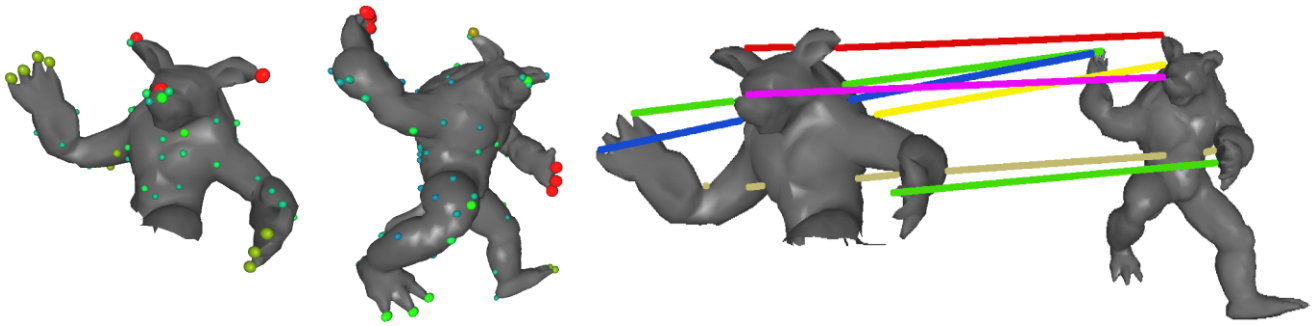

Fig. 1 Matching with salient spectral geometric features. The highlighted feature points are extracted in the spectrum domain generated directly form the triangles meshes. Notice that the two meshes are different in position, orientation, scale, pose, number of vertices, and triangulation. Furthermore, the *left* shape is only a "part" of the whole model. In order to clearly see the matching result, only some of the matched points are displayed

the local region to create a descriptor of the corresponding feature point. This descriptor is stable, invariant, and distinctive. Overall, the salient features are extracted globally and described and supported locally. They can be used for both global matching and partial matching. Figure 1 shows an example of partial matching with our salient spectral geometry features.

Our contributions in this paper are summarized as follows:

- Salient Spectral Geometric Features. We propose a method to extract salient spectral geometric features in the spectrum domain which is invariant to Euclidean transformations and isometric deformations. Describing and matching shapes with their salient features also conforms to the procedure of "coarse-to-fine" multiresolution analysis.
- Local Supports of Salient Features. The features are extracted with identified local "frequencies" which imply spatial scales of local support regions defining the features. That is to say, each salient feature finds its local support.
- Applications. The salient spectral features are very stable and distinctive. The shape representation built upon them may achieve a higher level of shape description. It can be easily applied to tasks such as shape corresponding and shape retrieval.

1.1 Prior work

There are a number of well studied global shape representations, such as moment [3, 17, 22], extended Gaussian image [6, 23], shape distribution [8, 18, 19], and shape harmonics [11]. These works showed great power in shape analysis. But matching with these global representations usually requires the data to be aligned or normalized. It can be determined whether two shapes are similar or not, or how similar they are with those global representations. However, it is difficult to obtain more matching details directly, such as part level similarity, correspondence or registration. These global representations also perform poorly in a "part-to-whole" matching. A part or a sub-shape is always considered as a quite different shape from its original shape by these methods. To decide a proper scale of the part to the whole shape is also a difficult task.

A part-to-whole matching is also considered as partial matching which is more general than the global one. Partial matching decides if a shape is a part of another one and where it should be located. It is often applied with matching local features. Gal et al. [4] proposed a partial matching method based on salient local features extracted from 3D surfaces. The salient features are extracted locally with an area growing algorithm following an empirical formula, and the descriptors are defined on the quadratic fitted surfaces based on the original meshes. There are also more rigorous scale space-based methods for extracting salient features [7, 13, 26]. Graph-based approach is another important solution to shape matching. For example, Reeb graph [5] and skeletal graph [9, 24] represent a shape with a graph, and turn the matching problem into the graph problem. A part-to-whole matching can be handled here with subgraph searching. However, the graph extracted from a shape is sensitive to topology. The tiny change of topology may result in quite different graphs.

In this paper, we analyze shapes based on their spectrums. Shape spectrum is a new topic in computer graphics during the recent years. Reuter [20] defined shape spectrum as the family of eigenvalues of the Laplace–Beltrami operator on a manifold, and used it as a global shape descriptor. Lévy [14] pointed out that Laplace–Beltrami eigenfunctions are "tools" to understand the geometry of shapes and discussed the properties of those eigenfunctions of the Laplace–Beltrami operator. Rustamov [21] proposed a modified shape distribution base on eigenfunctions and eigenvalues. Karni and Gotsman [10] used the projections

of geometry on the eigenfunctions for mesh compression. The Laplace–Beltrami spectrum is showing more and more power in shape analysis. It is proved to have many good invariant properties [20]. In this paper, we propose to extract salient geometric features in the domain of spectrum.

2 Salient spectral feature extraction

Given a 3D triangle mesh, we first analyze its Laplacian spectrum and represent the shape by a set of salient feature points with scale information in its spectrum. With their associated scales, local Laplacian spectra are calculated and assigned as local shape descriptors to the feature points.

2.1 Laplacian shape spectrum

In this section, we will review the theory of the Laplacian spectrum and describe how to compute it on a triangle mesh.

Let $f \in C^2$ be a real function defined on a Riemannian manifold M. The Laplace–Beltrami operator Δ is defined as

$$\Delta f = \operatorname{div}(\operatorname{grad} f), \tag{1}$$

where $\operatorname{grad} f$ is the gradient of f and div is the divergence on the manifold [2]. The Laplace–Beltrami operator is liner differential and can be calculated in local coordinates. Let ψ be a local parametrization of a sub-manifold of M such that $\psi : \Re^n \to \Re^{n+k}$, $g_{ij} = \langle \partial_i \psi, \partial_j \psi \rangle$, $G = (g_{ij})$, $W = \sqrt{\det G}$, $(g^{ij}) = G^{-1}$, where $i, j = 1, 2, \ldots, n$, $\langle , \rangle$ is the dot product, and det is the determinant. The Laplace–Beltrami operator then is defined on the submanifold as

$$\Delta f = \frac{1}{W} \sum_{i,j} \partial_i \left(g^{ij} W \partial_j f \right).$$

If $M \subset \Re^2$, the Laplace–Beltrami operator reduces to the Laplacian

$$\Delta f = \frac{\partial^2 f}{(\partial x)^2} + \frac{\partial^2 f}{(\partial y)^2}. \tag{2}$$

Consider the Laplacian eigenvalue equation

$$\Delta f = -\lambda f, \tag{3}$$

where λ is a real scalar. The spectrum is defined to be the eigenvalues arranged increasingly as $0 \le \lambda_0 \le \lambda_1 \le \lambda_2 \le \cdots \le +\infty$. In the case of a close manifold or an open manifold with a Neumann boundary condition, the first eigenvalue λ_0 will always be zero. The spectrum is an isometric invariant because it only depends on the gradient and divergence which are dependent only on the Riemannian structure of the manifold. After the normalization of the eigenvalues, shape can be matched regardless of the scales. The Laplace–Beltrami operator is Hermitian, so the eigenvectors corresponding to its different eigenvalues are orthogonal:

$$\langle \phi_i, \phi_j \rangle = \int_M \phi_i \phi_j = 0, \tag{4}$$

where $i \neq j$. A given function f on the surface can be expanded as

$$f = c_1 \phi_1 + c_2 \phi_2 + c_3 \phi_3 + \cdots, \tag{5}$$

where the coefficients are

$$c_i = \langle f, \phi_i \rangle = \int_M f \phi_i. \tag{6}$$

Equation (3) can be solved by the finite element method [20]. In our framework, 3D surface data are discrete triangle meshes. A discrete Laplace–Beltrami operator K [16] can be applied on the triangle meshes,

$$K(p_i) = \frac{1}{2A_i} \sum_{p_j \in N_1(p_i)} (\cot \alpha_{ij} + \cot \beta_{ij})(p_i - p_j), \tag{7}$$

where $N_1(p_i)$ includes all the vertices, p_j, belonging to one ring neighborhood of a vertex, p_i. α_{ij} and β_{ij} are the two angles opposite to the edge in the two triangles sharing the edge i, j, and A_i is the Voronoi region area of p_i.

For the whole vertices of a triangle mesh, a Laplace-Beltrami matrix can be constructed as:

$$L_{ij} = \begin{cases} -\frac{\cot \alpha_{ij} + \cot \beta_{ij}}{2A_i} & \text{if } i, j \text{ are adjacent,} \\ \sum_k \frac{\cot \alpha_{ik} + \cot \beta_{ik}}{2A_i} & \text{if } i = j, \\ 0 & \text{otherwise,} \end{cases} \tag{8}$$

where α_{ij}, β_{ij}, and A_i are the same as in (7) for certain i and j. Then, the spectrum problem (3) turns into the following eigenvalue problem:

$$L\vec{v} = \lambda \vec{v}, \tag{9}$$

where $\vec{v}$ is an n-dimensional vector. Each entry of $\vec{v}$ represents the function value at one of n vertices on the mesh. The equation above can be represented as a generalized eigenvalue problem which is much easier to solve numerically by constructing a sparse matrix M and a diagonal matrix S such that

$$M_{ij} = \begin{cases} -\frac{\cot \alpha_{ij} + \cot \beta_{ij}}{2} & \text{if } i, j \text{ are adjacent,} \\ \sum_k \frac{\cot \alpha_{ik} + \cot \beta_{ik}}{2} & \text{if } i = j, \\ 0 & \text{otherwise,} \end{cases}$$

and $S_{ii} = A_i$. Thus, the Laplace Matrix L is decomposed as $L = S^{-1}M$ and the generalized eigenvalue problem is presented as:

$$M\vec{v} = \lambda S \vec{v}. \tag{10}$$

As defined above, M is symmetric and S is symmetric positive-definite. All the eigenvalues and eigenvectors are real, and the eigenvectors corresponding to different eigenvalue are orthogonal in terms of S dot-product:

$$\langle \vec{u}, \vec{w} \rangle_S = \vec{u}^T S \vec{w}, \tag{11}$$

where $\vec{u}$ and $\vec{w}$ are eigenvectors of (10). Then (4), (5) and (6) can be reduced, respectively, to

$$\langle \vec{v}_i, \vec{v}_j \rangle_S = 0, \quad i \neq j, \tag{12}$$

$$\vec{f} = \sum_{i=1}^{n} \vec{v}_i c_i, \tag{13}$$

and

$$c_i = \langle \vec{f}, \vec{v}_i \rangle_S. \tag{14}$$

Under this setting, the spectrum, $\{0, \lambda_1, \lambda_2, \lambda_3, \ldots, \lambda_{n-1}\}$, is the family of eigenvalues of the generalized eigenvalue problem defined above.

2.2 Salient feature point detection

In this section, we will describe how to extract salient feature points based on the geometry and eigenfunctions since there is much shape information in the eigenvalues and eigenfunctions. Figure 2 illustrates some eigenfunctions on the armadillo model. The eigenfunctions contain very symmetric and meaningful information. Figure 3 shows isometric properties of eigenfunctions. They are the 5th eigenfunctions on different meshes. The three meshes are generated from the same shape with different poses. The sampling rates are also different. In Fig. 3, (a) has 1,000 vertices, (b) has 1,500, while (c) has 3,000. We can see that the eigenfunctions are independent to poses and triangulations.

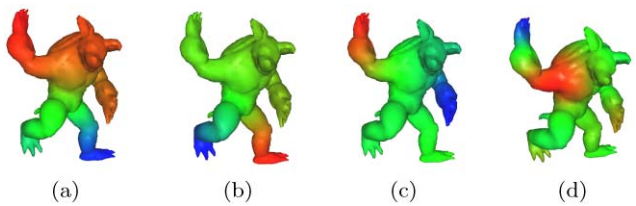

Fig. 2 The 2nd, 3rd, 4th, and 10th eigenfunctions on the shape. *Red color* indicates larger value while *blue color* denotes smaller value

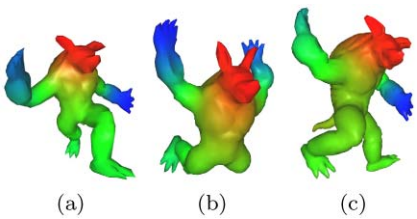

Fig. 3 The 5th eigenfunctions on the model with different poses. The eigenfunctions are isometrically invariant. The three shapes, *from left to right*, have 1000, 1500, and 3000 vertices, respectively

Consider the geometric reconstruction problem. Let matrix P be the position matrix consisting of the $\{x, y, z\}$ coordinates of each vertex:

$$P = [X, Y, Z], \tag{15}$$

where $X = [x_1, x_2, x_3, \ldots, x_n]^T$, $Y = [y_1, y_2, y_3, \ldots, y_n]^T$, and $Z = [z_1, z_2, z_3, \ldots, z_n]^T$ are coordinate vectors. Then the expansion with (13) and (14) can be rewritten in matrix form as:

$$P = VC^T, \tag{16}$$

where V is the eigenvector matrix $V = [v_1, v_2, \ldots, v_n]$ and $C = P^T SV$. Let $A_{1-p,1-q}$ denote a sub-matrix consisting of 1-p rows and 1-q columns of matrix A. Then the first k eigenfunctions' reconstruction is represented as:

$$P(k) = V_{1-n,1-k} C^T_{1-3,1-k}. \tag{17}$$

The reconstructed mesh is represented by the coordinate $P(k)$ with the same connections. Figure 4 shows a reconstruction process. The eigenfunctions corresponding with smaller eigenvalues represent lower frequency information. As more and more eigenfunctions are added up, more details of the mesh are presented. New salient features come out with new eigenfunctions, which means that features are contained by their eigenfunctions within the corresponding frequencies. We define the geometry energy of a vertex i corresponding with the kth eigenvalue as:

$$E(i,k) = \left\| V(i,k) \times C_{1-3,k} \right\|_2. \tag{18}$$

We pick the maxima in E as the feature points, which means more geometry energy is added locally in both spatial and spectral neighborhood. If $E(i,k)$ is larger than those of its neighboring vertices within several neighbor frequencies, it will be picked up as a salient feature point with a scale factor, $sf = 1/\sqrt{\lambda_k^2}$. Notice that, one vertex may be picked several times with different scale factors corresponding with different eigenvalues. See Fig. 5 for an example.

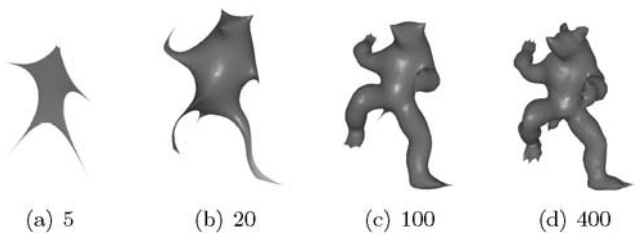

Fig. 4 Geometric reconstruction with the first 5, 20, 100, and 400 eigenfunctions, respectively

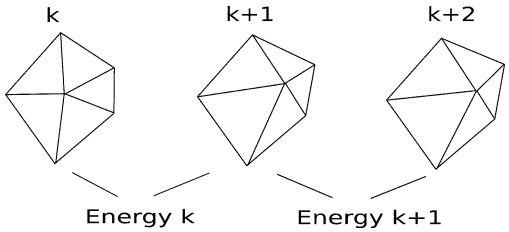

Fig. 5 Geometry energy between neighboring eigenfunction reconstructions. In this illustrative example, the vertex in the middle of the one ring neighborhood receives largest geometry energy when $(k+1)$th eigenfunction is added for reconstruction. Thus, it is considered as a maximum at the "frequency" of λ_k

2.3 Shape descriptor construction

In previous sections, we have described how feature points are extracted from an original mesh with scale information factors. The next step is to find a local descriptor for each feature point, which is invariant to translation, rotation, scaling, and isometric deformation, and also distinctive enough for similarity measure. We propose to use the Laplace–Beltrami spectrum of the spatial local region defined by the identified scale (i.e., the local support of the corresponding salient feature point). However, most of these regions are open boundary sub-surfaces and properties of those eigenfunctions of the Laplace–Beltrami operator. Rustamov [21] mentioned that the Laplace matrix could encounter some problems with an open boundary surface. In order to solve this problem, we attach another surface patch to the open boundary region patch. The attached patch has exactly the same shape as the original patch, but opposite normal at every point. Then, an open boundary path turns into a water-tight surface, and (10) can be applied on it without any problem.

The algorithmic procedure is as follow: First, a spatial local patch is extracted by drawing geodesic circle with the feature point as the center and $r \times 1/\sqrt{\lambda_k}$ as the radius, where r is a uniform, constant radius factor. Note that, because of the scaling factor, $1/\sqrt{\lambda_k}$, the shape of the local patch will remain the same despite the scaling of the mesh. Then, (10) is applied on the patch to obtain the spectrum of the patch. Finally, for similarity comparison, the spectrum is normalized by a fitting function $f(x) = \frac{4\pi}{A}x, x = 1, 2, \ldots, n$, where A is the area of the local patch [20]. Figure 6 illustrates how to construct a descriptor for a feature point. The histograms show the spectral values over the eigenvectors in the local patches. The matching can be performed by comparing the Euclidean distance between two descriptors.

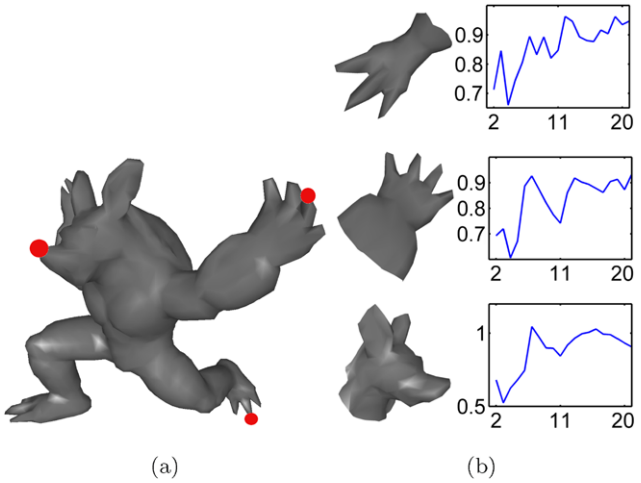

Fig. 6 The local shape descriptors of the model in (**a**) are normalized spectra of local patches as shown in (**b**)

3 Correspondence and matching

Given a 3D surface, we can now represent it with a set of salient spectral geometric features. In this section, we propose a method to build a correspondence between two models with those features. The correspondence problem can be described as: If there are two sets of features $\{p_i\}$ and $\{p'_{i'}\}$, try to find a mapping function $\phi(\cdot)$ such that $\phi(i) = i'$. The similarity between these two models relies on the mapping function ϕ. We denote the similarity as

$$\mathrm{Sim}(\phi) = \mathrm{Sim}_s(\phi) + \mathrm{Sim}_p(\phi), \tag{19}$$

where $\mathrm{Sim}_s(\phi)$ is the similarity calculated based on single-feature-to-single-feature mapping and $\mathrm{Sim}_p(\phi)$ based on cluster-to-cluster mapping. Single-to-singe feature similarity can be based on the Euclidean distances between the spectrum descriptors. Let $f(i)$ denote the feature vector of the feature i, then $\mathrm{Sim}_s(\phi)$ is defined as

$$\begin{aligned} \mathrm{Sim}_s(\phi) &= \omega_s \sum_{\phi(i)=i'} C(i,i'), \\ C(i,i') &= \exp\left(\frac{\|f(i) - f(i')\|^2}{2\sigma_s^2}\right). \end{aligned} \tag{20}$$

Cluster-to-cluster feature similarity is based on the relative geodesic distances and scale factors. Let $g(i,j)$ denote the absolute geodesic distance between i and j based on the spatial coordinate and let $sf(i)$ denote the scale factor of i, then $\mathrm{Sim}_p(\phi)$ is defined as

$$\begin{aligned} \mathrm{Sim}_p(\phi) &= \omega_p \sum_{\phi(i)=i', \phi(j)=j'} H(i,j,i',j'), \\ H(i,j,i',j') &= \exp\left(\frac{(d_{\mathrm{pg}}(i,j,i'j') + \beta d_{\mathrm{ps}}(i,j,i'j'))^2}{2\sigma_p^2}\right), \end{aligned} \tag{21}$$

where d_{pg} is the distance between relative geodesic distances

$$d_{\text{pg}}(i, j, i' j') = \left| \frac{g(i, j)}{sf(i)} - \frac{g(i', j')}{sf(i')} \right|, \tag{22}$$

and d_{ps} is the distance between scale ratios

$$d_{\text{ps}}(i, j, i' j') = \left| \log\left(\frac{sf(j)}{sf(i)}\right) - \log\left(\frac{sf(j')}{sf(i')}\right) \right|. \tag{23}$$

ω_s, σ_s, ω_p, σ_p, and β are weight scalars. The goal of the correspondence algorithm is to find certain mapping function ϕ_c which maximizes the similarity $\text{Sim}(\phi)$. If we define binary indicators variable $x(i, i')$ as

$$x(i, i') = \begin{cases} 1 & \text{if } \phi(i) = i' \text{ exists,} \\ 0 & \text{otherwise,} \end{cases} \tag{24}$$

then (19) can be represented by an Integer Quadratic Programming (IQP) problem as

$$\text{Sim}(x) = \sum_{i,i',j,j'} H(i, j, i', j') x(i, i') x(j, j') + \sum_{i,i'} C(i, i') x(i, i'). \tag{25}$$

We also constrain a one-to-one mapping, which means one feature in a model cannot be assigned more than one correspondence in the other model. Consequently, we have $\sum_i x(i, i') \leq 1$ and $\sum_{i'} x(i, i') \leq 1$. These linear constraints can be encoded in one row of A and an entry of b. Therefore, our IQP problem can be formalized in the following matrix form:

$$\max \text{Sim}(x) = x' H x + C x \quad \text{subject to } Ax \leq b. \tag{26}$$

We use the IQP solver proposed by Bemporad et al. [1] to solve the above optimization problem.

4 Experiments and applications

Salient spectral geometric features: In previous sections, we have introduced our method for extracting salient spectral geometric features from a surface. Figure 7 shows some examples of salient feature points. The vertices colored in red, green and blue colors are feature points extracted in the spectrum domain with our method. Each mesh in Fig. 7 has 1,000 to 1,500 vertices. In order to find extrema in the spectrum domain, each vertex is compared with its one-ring neighbors within three frequencies: the current, the previous, and the next. The extrema are extracted in the first 100 eigenfunctions. Redder color means the feature is found in a lower "frequency", which has large supporting region, while bluer color corresponds to higher "frequency". Only lowest "frequency" is visualized for a vertex with multi "frequencies". The highlighted patches illustrate the local supports for some identified feature points. The experiments show that the salient features are very stable and invariant to Euclidean transforms and isometric deformations.

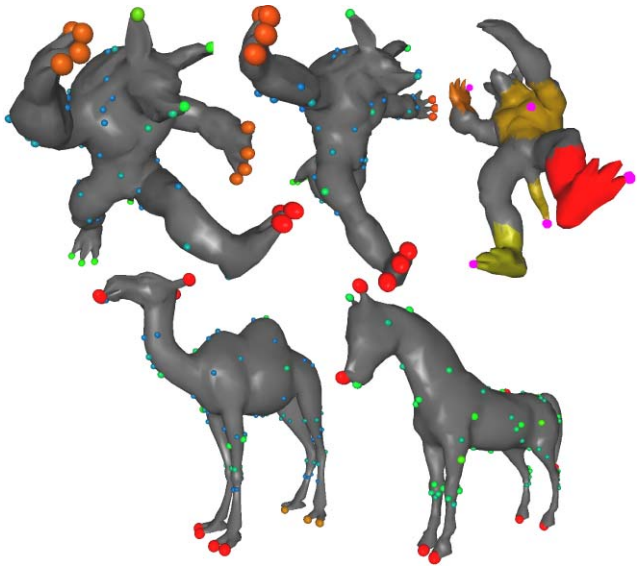

Fig. 7 Salient feature points extracted in the spectrum domain. *Redder color* means the feature is found in a lower "frequency", which has a large supporting region, while *bluer color* corresponds to a higher "frequency". The highlighted patches illustrate the local supports for some of the feature points

Shape correspondence: A nature application with the salient features is partial matching. Because each feature point is found with both the position and the scale factor, there is a local region to support the feature point. The ratio of the local support region to the entire surface is independent of the scale of the original surface. In our experiments, the radius constant r is set to be 1.7 and a geodesic circle patch is approximated with the graph shortest edge path on the mesh. Then, the spectrum of the local patch is calculated, and the descriptor consists of the eigenvalues of λ_1 to λ_{21} with normalization. Figures 1 and 8 show some examples of matching and partial matching. The two meshes in the matching pairs are different in position, orientation, scale, pose, and triangulation. Our experiments demonstrated that the salient features are very powerful in matching of similar shapes. In Fig. 8(a) and (b) are shapes of the same armadillo model with different poses. We can see that even poses are quite different from each other but the correspondences are stable, even at very detailed levels. Note that the mirrored matches could happen in our algorithm. Not only the different poses from the same model, but also similar shapes can have correct correspondences, too. Figure 8(c) illustrates a dog shape corresponding to a horse shape with their similar features, such as heads, knees, necks, and feet.

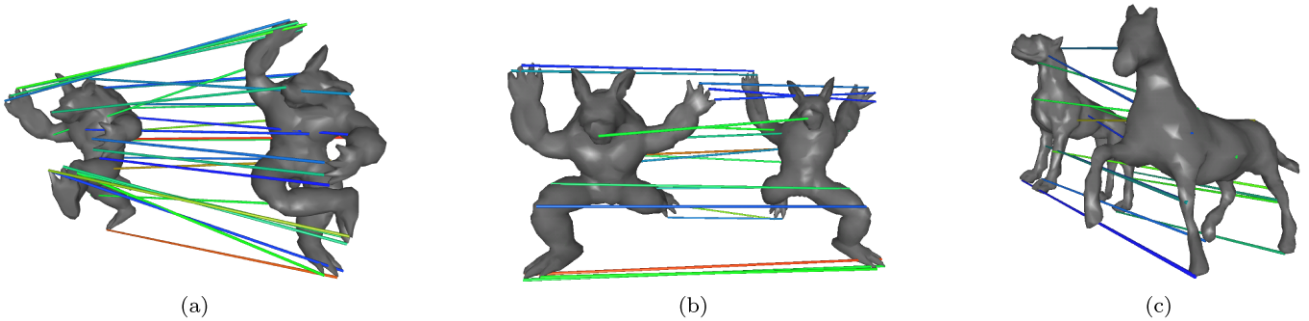

Fig. 8 Examples of matching. (**a**) and (**b**) demonstrate correspondence between shapes form the same model with different poses. (**c**) Shows correspondence between similar shapes

Fig. 9 Examples of shape retrieval with salient spectral geometric features. The 3D shapes at the *left-most column* are input queries, and those on the *right* are the first five retrieved results from the database

Shape retrieval: Another application is 3D shape searching and retrieval in large databases. Not only globally, shape can also be searched by parts, which leads to a more powerful partial matching. We use SHREC '07 3D shape database. We extract 10 shapes from each category. Since our framework extracts stable and distinctive salient spectral geometric features, the retrieval task is very straightforward by comparing the matching score of the IQP throughout the database, and then picking up the best ones as the query outputs. Figure 9 shows some results demonstrating the stability and accuracy of our retrieval. For the dataset that we use,

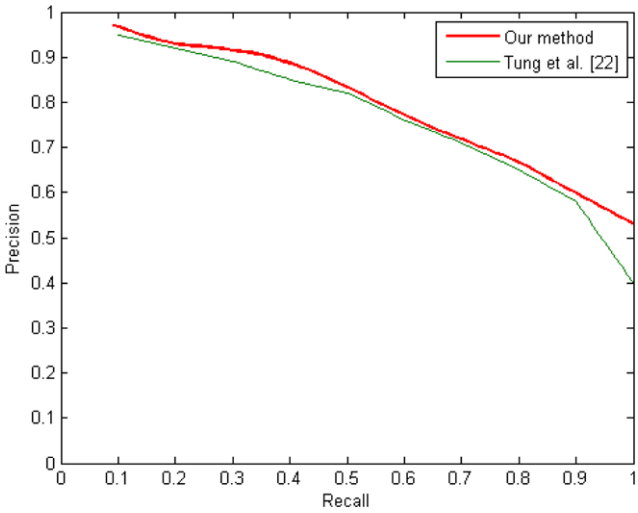

Fig. 10 The overall averaged precision/recall graph of our method on the SHREC datasets and its comparison to the method by Tung et al. [25]

our method outperforms the reported best result in the latest SHREC contest [25]. Figure 10 shows the precision/recall graph.

As we mentioned in the previous sections, another desirable property of the salient spectral geometric features is their powerful partial representation. Figure 11 shows how our method performs in retrieving shapes if only a part is given.

5 Conclusion

We have introduced a novel 3D shape representation with a set of salient feature points in the Laplace–Beltrami spectrum. The spectrum is defined as the family of eigenvalues of the Laplace–Beltrami operator on a manifold. The eigenvalues and eigenfunctions are invariant to translation, rotation, and scaling. They are also invariant to isometric transformations. We have introduced how to calculate the spectrum directly on triangle meshes. The results showed the spectrum

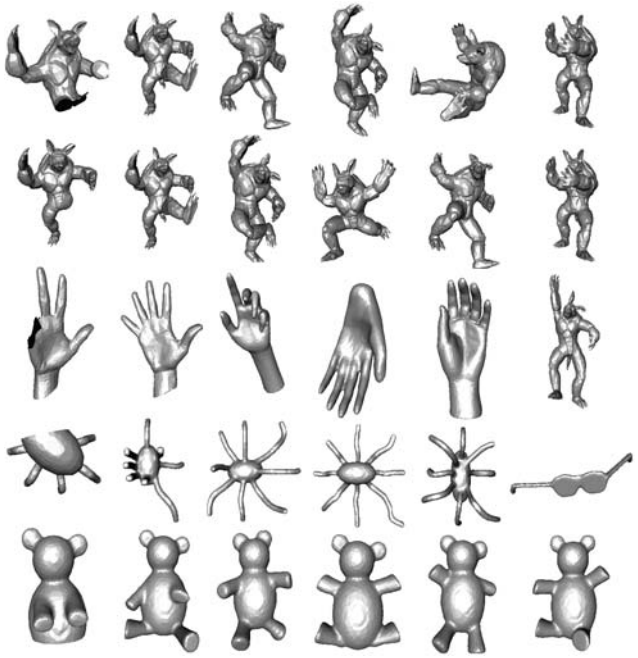

Fig. 11 Examples of partial shape retrieval with salient spectral geometric features. The shapes at the *left-most column* are input queries, and those on the *right* are the first five retrieved results from the database

relies only on the geometry of the manifold. It is very stable under Euclidean and isometric transformations and is independent of different triangulations. The spectrum energy domain is obtained by projecting the geometry onto the eigenfunctions. The salient features are the energy maxima in the geometry energy domain. The salient features share the nice properties of the Laplace-Beltrami spectrum. The maxima provide not only where the features are on the manifold but also the "frequency" where the features lie in. A scale of a local region can be determined with the "frequency" to support a feature point. With the IQP algorithm, correspondences can be built among variant shapes in very detailed levels. Salient spectral feature point representation is ideal for fundamental shape matching. Our experiments show its great power in shape retrieval and searching. Besides global matching, partial matching is also supported in our framework.

Although our experiments have shown the great power of salient spectral feature, there can still be some future work to improve its performance. For example, mirror effects sometimes affect the accuracies of detailed correspondences. High level clustering and matching algorithms could be employed to overcome those problems. Also, our current framework used graph shortest path to approximate the geodesic distance when drawing a geodesic circle on the mesh. The error may be reduced when a more accurate geodesic algorithm is applied.

Acknowledgements The authors would like to thank for the 3D surface data provided in SHREC '07 database. This work is supported in part by the research grants: NSF IIS-0713315, NSF CNS-0751045, NIH 1R01NS058802-01A2, and NIH 2R01NS041922-05A1.

References

1. Bemporad, A., Mignone, D., Morari, M.: An efficient branch and bound algorithm for state estimation and control of hybrid systems. In: Proceedings of European Control Conference (1999)
2. Chavel, I.: Eigenvalues in Riemannian Geometry. Academic Press, San Diego (1984)
3. Duda, R.M., Hart, P.E.: Pattern Classification and Scene Analysis. Wiley, New York (1973)
4. Gal, R., Cohen-Or, D.: Salient geometric features for partial shape matching and similarity. ACM Trans. Graph. **25**(1), 130–150 (2006)
5. Hilaga, M., Shinagawa, Y., Kohmura, T., Kunii, T.L.: Topology matching for fully automatic similarity estimation of 3D shapes. In: Proceedings of the 28th Annual Conference on Computer Graphics and Interactive Techniques, pp. 203–212 (2001)
6. Horn, B.K.P.: Extended Gaussian images. In: Proceedings of IEEE, vol. 72, pp. 1671–1686 (1984)
7. Hua, J., Lai, Z., Dong, M., Gu, X., Qin, H.: Geodesic distance-weighted shape vector image diffusion. IEEE Trans. Vis. Comput. Graph. **14**(6), 1643–1650 (2008)
8. Ip, C., Lapadat, D., Sieger, L., Regli, W.C.: Using shape distributions to compare solid models. In: Proceedings of ACM Symposium on Solid Modeling and Applications, pp. 273–280 (2002)
9. Iyer, N., Kalyanaraman, Y., Lou, K., Jayanti, S., Ramani, K.: A reconfigurable 3D engineering shape search system: Part I: Shape representation. In: Proceedings of ASME Computers and Information in Engineering Conference, pp. 1–10 (2003)
10. Karni, Z., Gotsman, C.: Compression of soft-body animation sequences. Comput. Graph. **28**(1), 25–34 (2004)
11. Kazhdan, M., Funkhouser, T., Rusinkiewicz, S.: Rotation invariant spherical harmonic representation of 3D shape descriptors. In: Proceedings of the ACM/Eurographics Symposium on Geometry Processing, pp. 167–175 (2003)
12. Kendall, D.G.: The diffusion of shape. Adv. Appl. Probab. **9**(3), 428–430 (1977)
13. Lee, C.H., Varshney, A., Jacobs, D.W.: Mesh saliency. ACM Trans. Graph. **24**(3), 659–666 (2005)
14. Lévy, B.: Laplace–Beltrami eigenfunctions: Towards an algorithm that understand s geometry. In: Proceedings of IEEE International Conference on Shape Modeling and Applications, p. 13 (2006)
15. Marr, D.: Vision: A Computational Investigation into the Human Representation and Processing of Visual Information. Freeman, New York (1982)
16. Meyer, M., Desbrun, M., Schröder, P., Barr, A.: Discrete differential geometry operators for triangulated 2-manifolds. In: Proceedings of the VisMath Conference, pp. 1–26 (2002)
17. Novotni, M., Klein, R.: 3D zernike descriptors for content based shape retrieval. In: Proceedings of ACM Symposium on Solid Modeling and Applications, pp. 216–225 (2003)
18. Ohbuchi, R., Takei, T.: Shape-similarity comparison of 3D models using alpha shapes. In: Proceedings of the 11th Pacific Conference on Computer Graphics and Applications, pp. 293–302 (2003)
19. Osada, R., Funkhouser, T., Chazelle, B., Dobkin, D.: Shape distributions. ACM Trans. Graph. **21**(4), 807–832 (2002)
20. Reuter, M., Wolter, F.E., Peinecke, N.: Laplace–Beltrami spectra as "Shape-DNA" of surfaces and solids. Comput. Aided Des. **38**(4), 342–366 (2006)

21. Rustamov, R.M.: Laplace–Beltrami eigenfunctions for deformation invariant shape representation. In: Proceedings of the Fifth Eurographics Symposium on Geometry Processing, pp. 225–233 (2007)
22. Sadjadi, F.A., Hall, E.L.: Three-dimensional moment invariants. IEEE Trans. Pattern Anal. Mach. Intell. **2**(2), 127–136 (1980)
23. Shum, H., Hebert, M., Ikeuchi, K.: On 3D shape similarity. In: Proceedings of IEEE Conference on Computer Vision and Pattern Recognition, pp. 526–531 (1996)
24. Sundar, H., Silver, D., Gagvani, N., Dickinson, S.: Skeleton based shape matching and retrieval. In: Proceedings of IEEE International Conference on Shape Modeling and Applications, pp. 130–139 (2003)
25. Tung, T., Schmittt, F.: Shape retrieval of noisy watertight models using aMRG. In: Proceedings of IEEE International Conference on Shape Modeling and Applications, pp. 229–230 (2008)
26. Zou, G., Hua, J., Dong, M., Qin, H.: Surface matching with salient keypoints in geodesic scale space. J. Comput. Animat. Virtual Worlds **19**(3–4), 399–410 (2008)

Jiaxi Hu is a Ph.D. student at Wayne State University. He is currently a member of Graphics and Imaging Laboratory. He got his M.S. degree and B.S. degree from Huazhong University of Science and Technology at Wuhan, China in 2005 and 2003, respectively. His current research interests are geometric computing, computer graphics and scientific visualization.

Jing Hua is an assistant professor of Computer Science at Wayne State University and the director of Graphics and Imaging Lab (GIL). He received his Ph.D. degree (2004) and M.S. degree (2002) in Computer Science from the State University of New York at Stony Brook. His research interests include Computer Graphics, Visualization, 3D Image Analysis and Informatics. He has published over 80 peer-reviewed papers in the above research fields at top journals and conferences. He is currently the Principal Investigator/Co-Principal Investigator of research projects funded by the National Science Foundation, National Institutes of Health, Michigan Technology Tri-Corridor, 21st Century Jobs Funds, and WSU Research Foundation. Dr. Hua serves as an Editorial Board Member for International Journal of Technology Enhanced Learning, Scientific Journals International and Journal of Digital Culture as well as a Program Committee Member for many international conferences. He is a member of IEEE.